Damage Analysis of Chemically Corroded Sandstone Under Cyclic Impact and Static Axial Pressure

Zhuyu Zhao
JiangXi University of Science and Technology
Jinchun Xue (exampie19951123@163.com)
JiangXi University of Science and Technology https://orcid.org/0000-0001-8519-4534
Jiefang JIN
JiangXi University of Science and Technology
Li Tan
JiangXi University of Science and Technology
Ruoyan Cai
JiangXi University of Science and Technology
Wenbin Xia
Jiangxi University of Science and Technology School of Energy and Mechanical Engineering

Research Article

Keywords: Cyclic impact, Axial compression, Chemical corrosion, Strength characteristics, Failure form

Posted Date: May 28th, 2021

DOI: https://doi.org/10.21203/rs.3.rs-479247/v1

Version of Record: A version of this preprint was published at Geotechnical and Geological Engineering on January 10th, 2022. See the published version at https://doi.org/10.1007/s10706-022-02047-3.

Damage analysis of chemically corroded sandstone under cyclic impact and static axial pressure

Zhuyu Zhao [a], Jinchun Xue[a,*], Jiefang JIN [b], Li Tan [a], Ruoyan Cai [a], Wenbin Xia [a]

[a] School of Energy and Mechanical Engineering, Jiangxi University of Science and Technology, Nanchang, Jiangxi 330013, China

[b] Jiangxi Provincial Key Laboratory of Environmental Geotechnology and Engineering Disaster Control, Ganzhou, Jiangxi 341000, China

Abstract

To explore the influence of cyclic impact and axial pressure on the damage of chemically corroded sandstone, a series of cyclic impact tests were carried out on white sandstone by using Split Hopkinson Pressure Bar. The longitudinal sections and fractures of samples were observed with the scanning electron microscope. The aim was to investigate the damage characteristics and structural changes of sandstone, that subjected to the coupling of force and chemistry. The results show that: (1) When pH of solution is 7, the total cyclic impact number and stress peak of specimens both became larger, and the rock samples responded with a significantly high resistant strength. (2) The stress wave transmission coefficient of sandstone decreases gradually with the increase of the number of cyclic impacts, while the reflection coefficient shows a tendency of" decreasing first and then increasing". (3) Cylindrical specimens with a certain axial pressure present an "X" shaped conjugate failure under cyclic impact. When axial pressure is too large or excessive impact, the "X" shaped conjugate undergoes shear to a state of broken cone. (4) The vertical section and fracture surface damage degree of white sandstone soaked in Na_2SO_4 solution is more serious than that in NaCl solution.

Keywords: Cyclic impact; Axial compression; Chemical corrosion; Strength characteristics; Failure form

1. Introduction

With the exploitation of resources and large-scale construction of infrastructures, mining industry, water conservancy and hydropower, traffic engineering and earthwork excavation are inseparable from geotechnical engineering[1]. The stability of rock is affected by static stress and external frequent vibration. Besides, in the design, construction, and management process of engineering, it is inevitable to consider the influence of complex hydro chemical field on rocks, which is caused by the discharge of domestic sewage and industrial wastewater. It is of significance to investigate the coupling of force and chemical corrosion for the long-term stability of geotechnical engineering. Recently, experts at home and abroad have carried out corresponding studies on the mechanical behavior that rock subjected to cyclic loading or chemical corrosion by theoretical derivation, simulation calculation, scientific experiments [2-6].

Based on the need for deep rock research, Li et al. [7] took the lead in putting forward the subject about the stability of rock under dynamic and static loading. He pointed out that when static axial pressure increases from 0 to 70% of the uniaxial static pressure strength, constant impact dynamic loading, the strength of rock in static loading or pure dynamic loading is less than that under the combined loading. Hu et al. [8] used a high-speed camera to record the compression fracture process of cylindrical red sandstones (d=50mm, h=50mm) subjected to the dynamic impact of Split Hopkinson Pressure Bar (SHPB). They divided the influence of cyclic loading incident energy for failure state of rock specimens into three stages: complete, crack, and broken. Gong et al.[9] put forward the tendency index for rock burst subjected to dynamic and static loading, which can efficaciously reflect static and dynamic loading on the occurrence of prompting rock burst. Jin et al.[10] performed a series of cyclic loading tests on sandstone subjected to different static loading by SHPB, and found that a combination form of static loading has influences on the failure mode of rock under cyclic impact, such as no end effect without static axial loading. Yin et al. [11] performed impact loading experiments on granite under the combined function of temperature and axial pressure loading through improved SHPB, and observed the internal structural characteristics of rock fragments with scanning electron microscope（SEM）. Tang et al. [12]carried out uniaxial compressive tests on three types

*Corresponding author at: School of Energy and Mechanical Engineering, Jiangxi University of Science and Technology, Nanchang, Jiangxi 330013, China.
E-mail address: 1023817019@qq.com

of rocks (granite, red sandstone, and limestone) in the hydrochemical environment, and uniaxial strength reduction of rocks represents the chemical damage of rocks. The results showed that the chemical damage of rocks is directly proportional to the chemical reaction strength of water-rock. Wei et al. [13] considered the mechanism of fractal dimension of rock, and concluded that fractal dimension is linearly proportional to the damage degree of chemical corrosion. Wu et al. [14] carried out rock dynamic mechanical tests on SHPB test system, and studied the dynamic mechanism of rock burst through energy theory. Feng et al. [15] conducted a full-process compression test on the multi-crack limestone under the chemical environment through a newly developed microscopic loading instrument, and obtained the deformation characteristics of specimens, the expansion process of cracks, and rock bridge bonding mode during failure.

In summary, studies cited above primarily focus on chemical corrosion damage mechanisms or the mechanical properties of rock impact under single factor conditions. However, few studies have addressed rock samples subjected to cyclic loading under the coupling function of chemical corrosion and static axial loading. Combined with the one-dimensional stress wave theory, the improved SHPB was utilized to investigate the white sandstone soaked in different hydrogen ion concentration index chemical solutions and different axial pressures. The mechanism of impact strength weakening and structural damage of white sandstone are discussed under multi-factor coupling. It provided a theoretical basis for safe and efficient construction management of rock blasting engineering under complex geological conditions.

2. Experimental Study

2.1 Sample Preparation

White sandstone, a common sedimentary rock in Kunming, was selected as the test object in this experiment. The white sandstone blocks, which was selected from a good homogeneity and integrity sample, were machined into cylindrical shapes with a length of 50 mm and a diameter of 50 mm according to the relevant guidelines of International Society for Rock Mechanics (ISRM) [16]. ln the meantime, to reduce the specimen accuracy effect on the test results, both sides of the specimens were polished with the sandpapers to ensure that the unevenness and non-perpendicularity were within ± 0.02 mm. Some prepared samples that would be tested were summarized in Fig.1 and Fig.2. The processed specimens were vacuum dried and sealed in 8 groups of chemical solutions for 240 days. The specific chemical solution is shown in Table1.（The influence of temperature and hydrogen ion concentration index of chemical solution over time was not considered during the immersion process.）

Table 1 Chemical solution

Solute composition	Concentration /mol•L^{-1}	pH
NaCl	0.1	2、7、9、12
Na_2SO_4	0.1	2、7、9、12

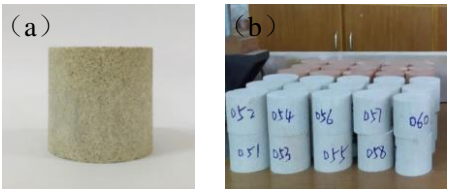

Fig.1 White sandstone specimens

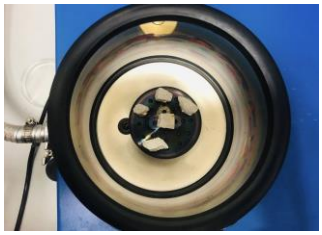

Fig.2 Scanning electron microscope of samples

2.2Equipment

The paper has two main tests. Cyclic impact tests refer to the cyclic impact load applied to the white sandstone specimen immersed in the chemical solution. Cyclic impact tests were carried out at Jiangxi Provincial Key Laboratory of Environmental Geotechnology and Engineering Disaster Control. The Split Hopkinson Pressure Bar experimental system mainly consists of the following: launch system; infrared velocity measurement system; three elastic bars with a 50mm rod diameter (the incident bar, transmitted bar, and bumper bar); strain data-collecting system and axial loading system. The elastic bars were made of high strength 40 Cr alloy steel with a density of 7.81g/cm^3, and a P-wave velocity of 5410 m/s. The lengths of the input bar, the output bar, and the bumper bar are 2000mm, 1500mm, and 300mm. The device diagram is shown in Fig. 3.

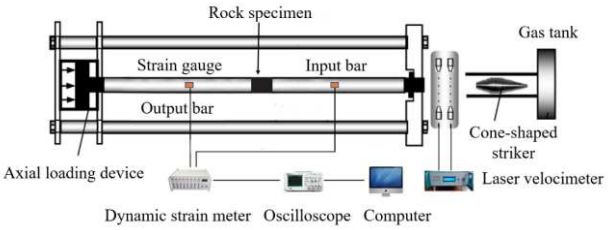

Fig.3 Diagram of SHPB testing apparatus

The other is a scanning electron microscope, which compared the longitudinal section and fracture surface of the specimen after impact. SEM was performed by Zeiss EVO18 scanning electron microscope in Germany. The tungsten filament in the electron gun is placed in the heat excited state by high voltage, which generates a focused high-energy electron beam to scan the surface of specimens. It is exciting the secondary electrons, backscattered electrons, and other physical signals, which are collected, amplified, and modulated into images. The real object is shown in Fig.4.

Fig.4 Scanning electron microscopy

2.3 Test Scheme

Before the impact tests started, a uniaxial compressive strength test by the RMT-150C rock mechanics testing machine is necessary to provide a reference for the axial pressure of subsequent impact tests. The physical and mechanical parameters are shown in Table 2.

Table 2 Physical and mechanical parameters of specimens

Density /kg·m^{-3}	Loading rate /MPa•s^{-1}	Strain rate /s^{-1}	Static loading compressive strength /MPa	Secant modulus /GPa	Poisson's ratio
2321	0.23	1.00×10^{-5}	31.5	17.65	0.25

The cyclic impact tests were performed at the following axial pressures: 20%, 40%, 65%, and 85% of uniaxial compressive strength, which were 6.3MPa、12.6MPa、20.5MPa, and 26.8MPa. Considering the upper and lower limits of the action density of stress wave propagating energy in rock [17], the pressure of the high-pressure gas chamber was set at 0.8 MPa, and the position of the cone-shaped striker in the launching cavity was fixed. Keeping the impact velocity at about 4.5m/s, the half sine wave achieved the purpose of constant strain rate load.

The steps of impact test are as follows:

①To ensure the energy conservation of equipment and bars, it is necessary to carry out an impact test without a test piece. ② The specimen is clamped between two rods, and vaseline is applied on both ends to reduce friction. ③Adjust the oil pump and apply the predetermined axial pressure slowly and uniformly. ④ Release nitrogen in the gas chamber and apply impact loading. ⑤Check, record, and photograph the state of specimens after impact. This is repeated until the specimen can no longer carry the loading.

The steps of electron microscope test are as follows:

①Samples are taken from the longitudinal section and fracture surface of the specimen. ② Clean the surface of the specimen with air blowing. ③ The samples are sprayed with gold film by an ion sputtering instrument. ④ According to the suggestion of magnification, from the sample preparation and geological application of SEM [18], the image is magnified by 100 and 1000 times.

2.4 Test Principle

To obtain the dynamic stress-strain curves, adopting the three-wave theory is widely used owing to its accuracy [19].Combined with the one-dimensional stress wave theory, the stress σ_t, strain ε_t, and average strain rate$\dot{\varepsilon}_t$ of the specimen can be calculated in the light of the following equations:

$$\sigma_t = \frac{A_e E_e}{2A_s}[\varepsilon_I(t) + \varepsilon_R(t) + \varepsilon_T(t)] \qquad (1)$$

$$\varepsilon_t = \frac{C_e}{L_s}\int_0^t [\varepsilon_I(t) - \varepsilon_R(t) - \varepsilon_T(t)]\,\mathrm{dt} \qquad (2)$$

$$\dot{\varepsilon}_t = \frac{C_e}{L_s}[\varepsilon_l(t) - \varepsilon_R(t) - \varepsilon_T(t)] \quad (3)$$

where A_e and A_s are the cross-sectional area of elastic rod and rock specimen; L_s is the length of the specimen; E_e is the elastic modulus of the elastic bar; Ce is longitudinal wave velocity; $\varepsilon_l(t), \varepsilon_R(t), \varepsilon_T(t)$ denote the incident, reflected, and transmission pulse signals, respectively.

3.Test Results

A group of representative specimen parameters and test data are listed, as shown in Table 3. The strength of white sandstone is weakened by cyclic impact under the combined action of static axial pressure and chemical corrosion. The total cyclic impact number of specimens that can withstand the loading gradually decreases with the polarization of the hydrogen ion concentration index of the solution under the same axial pressure. When the hydrogen ion concentration index of the solution is 7, the total cyclic impact number and stress peak of specimens become larger, and the rock samples respond with a significantly high resistant strength. Under the same cyclic impact loading, the total cyclic impact number of specimens gradually decreases with the increase of axial pressure.

3.1 Wave propagation characteristics in white sandstone under cyclic impact loading

Stress wave characteristics of No. w-033 sample is taken as an example. Fig.5 shows the waveform superposition diagram of the cyclic impact process. From Fig. 5, it can be concluded that the peak of incident wave is the same, which is characterized by an identical overlapping waveform under cyclic impact loading. As the number of impacts increasing, the waveforms of transmission and reflection waves have no obvious change. However, the peak of transmission wave decreases gradually, while the peak of reflected wave increases, and the change of shock extreme value is more obvious in the later stage.

The transmission coefficient is defined as the peak ratio transmitted wave and incident wave in the waveform, and so is reflected wave [20]. Therefore, Eq. （4）、（5）can be simplified as follow:

$$R = \frac{|\varepsilon_T(t)|_{max}}{|\varepsilon_l(t)|_{max}} \quad (4)$$

$$T = \frac{|\varepsilon_R(t)|_{max}}{|\varepsilon_l(t)|_{max}} \quad (5)$$

Table 3 Parameters of specimens and test data

No.	Axial pressure /MPa	length /mm	Diameter /mm	Density/kg•cm^{-3}	pH	σ_f /MPa	σ_{max} /GPa	The number of cycle impact
w-062	6.3	47.03	49.08	2315	2	39.64	43.51	7
w-052		47.05	49.09	2329	7	43.12	43.20	9
w-033		47.06	49.11	2312	9	42.68	42.68	8
w-042		47.06	49.09	2322	12	42.03	49.43	7
w-063	12.6	47.05	49.12	2327	2	37.16	41.42	5
w-053		47.06	49.09	2312	7	51.56	51.56	8
w-034		47.05	49.09	2322	9	49.61	49.61	6
w-043		47.07	49.10	2328	12	39.87	50.10	5
w-064	20.5	47.06	49.14	2312	2	38.46	38.46	4
w-054		47.08	49.13	2329	7	43.11	43.11	5
w-037		47.05	49.10	2329	9	40.72	40.72	5
w-044		47.05	49.04	2320	12	40.75	42.83	2
w-065	26.8	47.06	49.12	2308	2	27.26	31.92	2
w-055		47.06	49.05	2329	7	32.01	32.01	3
w-036		47.06	49.06	2318	9	28.82	30.51	3
w-045		47.07	49.02	2317	12	25.71	29.98	2

Note: σ_f is first impact stress peak; σ_{max} is maximum stress peak of cyclic impact.

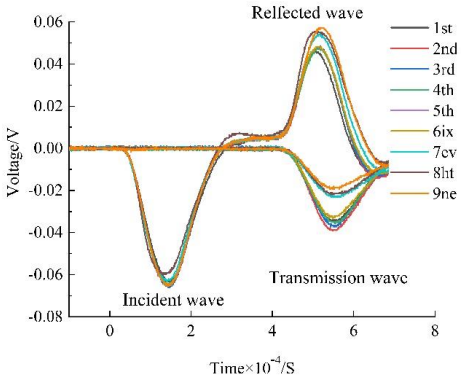

Fig.5 Stress wave superposition diagram of w-033

The transmission coefficient gradually decreases with the increase of the number of cyclic impacts, but the reflection coefficient has a trend of "first decrease and then increase" at point A. Because of the closure of primary fractures and the compaction of rocks in samples at the beginning of the impact that caused the increase of stress waves penetrability. From Fig. 6, it can be seen that the ability to reflect was the largest at point A under axial pressure of 12.6 MPa, compared with other axial pressures. Axial pressure not only play a mechanical role, such as expanding stress of pore and swelling stress of matrix, but also exhibit the formation of more microfractures in samples, which weaken its overall strength. Therefore, it can be summarized that the propagation coefficient of the wave was closely related to axial static.

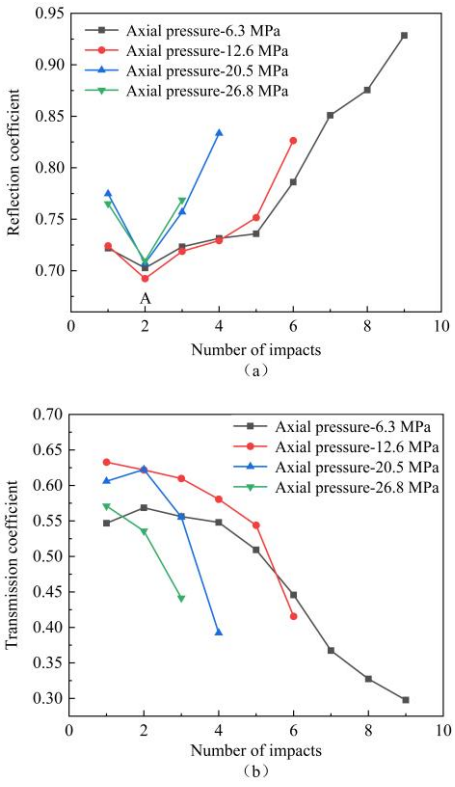

Fig.6 Trend chart of transmission and reflection coefficient

The rock mass is not completely homogeneous. Under cyclic impact load, the complete deformation of crack and joint is also nonlinear [21].The cracks and joints of rock are continuously activated and grow in the process of multiple impact. The stiffness and wave impedance of the joints will decrease with the increase of joints times. The ratio of joint closure to maximum joint closure decreases, and the cumulative damage of the specimen increases gradually. Therefore, the transmission and reflection coefficients of stress wave propagation at the interface of nonlinear crack and jointed rock can be calculated according to Eq. (6) (7) [22].

$$R = \frac{1}{\sqrt{1+4[\frac{K_0}{\omega Z(1-\gamma)^2}]^2}} \quad (6)$$

$$T = \frac{2}{\sqrt{4+[\frac{\omega Z(1-\frac{d}{d_m})^2}{K_0}]^2}} \quad (7)$$

where R and T are the reflection coefficient and transmission coefficient of stress wave propagating at the nonlinear joint; K_0 is the initial stiffness of the joint; ω is the frequency of stress wave; $Z = \rho C_P$ is the wave impedance of the specimen; $\gamma = \frac{d}{d_m}$ is the ratio of joint closure to maximum joint closure.

3.2 The strength characteristics of white sandstone under cyclic impact loading

Stress peak is an important indicator for measuring the strength characteristics of rock and can be applied to characterize the anti-compressive ability of rock under cyclic impact loading[21]. As shown in Fig. 7, sixteen typical specimens were tested and the trend of stress peak can be obtained during cyclic impact process. The stress peak of the specimens, in the early stage, change steadily under the axial pressure of 6.3Mpa, which is caused by the slow development and small damage degree of the micro-cracks in the rock. The stress peak decreases rapidly with the increase of impact times, in the later stage, due to the crack and joint propagation, the macroscopic failure occurs after repeated impact. The overall resistance capacity of external impact shows a trend of "stable in the early stage and sharply decreased in the later stage". The rate of decline of stress peak decline with increasing cycle impact number, compared

with axial compression of 6.3MPa, is the biggest for axial compression of 12.6MPa、20.5MPa. It may be that the application of high axial pressure exerts a destructive effect on the weak bedding surfaces and microcracks inside the rock, thereby aggravating cumulative damage of the rock during the process of cyclic impact. For axial compression of 26.8Mpa, dynamic stress peak of rock and impact times are more affected by the axial pressure, and the deformation of the rock is obvious, so internal damage is so great that it can't bear multiple impact loading.

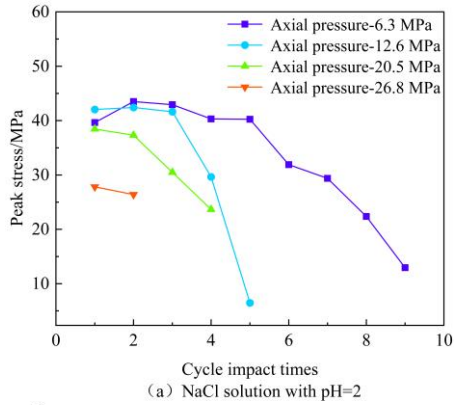

（a）NaCl solution with pH=2

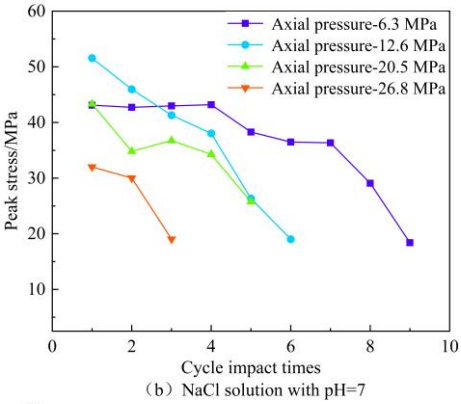

（b）NaCl solution with pH=7

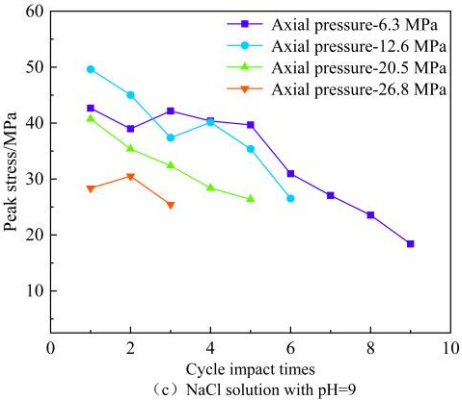

（c）NaCl solution with pH=9

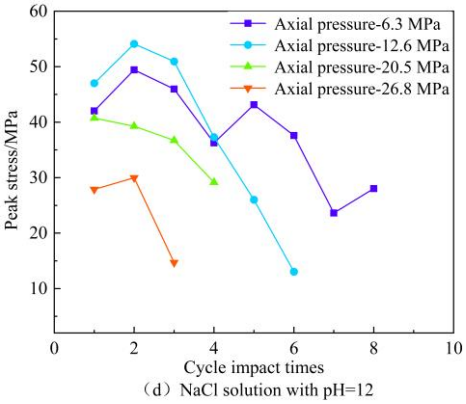

（d）NaCl solution with pH=12

Fig.7 Relationship between peak stress and the number of impacts under different axial pressures

Under the axial pressure of 12.6 MPa, stress peaks of the specimens are 42.03 MPa, 51.56 MPa, 49.61 MPa, and 47.01 MPa respectively, which are greater than those under other axial pressures. It indicates that the primary voids tend to close under the coupling function of the first impact and 12.6 MPa axial pressure, and the ability of the specimens to resist external impact compression is enhanced. Dynamic strength decreases more rapidly at higher axial pressures than that at lower axial pressures in the later period, which indicate that axial pressure intensified the accumulation of internal damage caused by the impact in the later period, and the ability to resist external impact deteriorate in the later period.

3.3 Dynamic failure characteristics of white sandstone under cyclic impact loading

The failure mode of specimens can directly reflect the macroscopic failure mode and microscopic damage mechanism of white sandstone under cyclic impact loading, which is of great significance for the analysis of rock impact state. Under different static axial loadings, impact loading, and chemical corrosion, the white sandstone samples fail mainly due to the formation of crack in the action of force. The size of axial pressure has a great influence on the mode and degree of specimen failure [24]. As shown in Fig. 8, the states of the specimens after impact can be divided into two categories, namely, "X" hyperbolic conjugate state and broken cone state. The "X" hyperbolic conjugate state is defined as an "X" shaped specimen that can withstand the loading after impact, as shown in Fig. 9 (a)and(b). The transverse ultimate tensile strain and oblique shear strength of rock are insufficient, and two ends of the

specimens are subjected to "X" conjugate hyperbolic failure along the oblique section. Consequently, the failure is mainly tensile shear failure. There are many local fissures near the middle of the failure on white sandstone with "X" shaped, which are not noticeable on both ends. The reason for this phenomenon is that smaller lateral constraints create the rock damage and generates more local micro-cracks near the middle of the failure on white sandstone specimens, which fully develop and merge into new fractures in the impact loading process. Few fractures are subject to large lateral restraint at both ends of the white sandstone specimen. The broken cone state refers to the state in which the specimen produced visible cracks after impact and separated into two cone bodies, as illustrated in Fig. 9 (c). The broken cone state is mainly caused by high axial pressure or multiple impacts in the same directions. This result indicates that the impact loadings and static axial loading played the dominant role in the failure of white sandstone sample. According to the theory of the maximum shear stress of the inclined section[25], the angle of shear dislocation surface is about 45 degrees. However, the incomplete homogeneity of the material and random orientations of cracks, the angle of the fracture surface is largely affected by two factors under cyclic impact loading. One of the internal reasons is that the rock is actually heterogeneous, and the angle of the fracture surface is affected by the nonlinear deformation of the cracks. Secondly, "X" shape is a non-holonomic regular solid, and the angle deviation will be produced when the load is applied instantaneously.

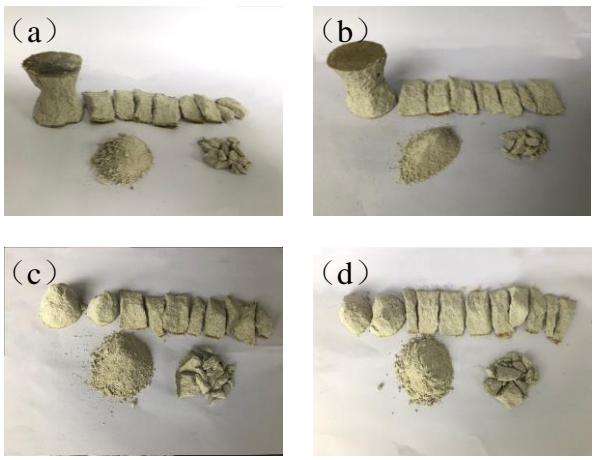

Fig.8 Failure mode of samples

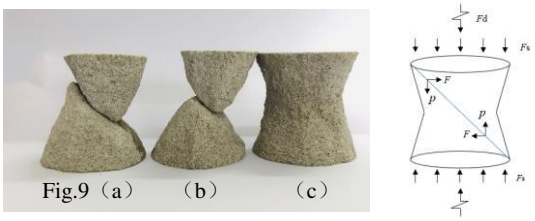

Fig.9 Failure modes and force condition of rocks

Electron microscope tests were carried out to study the effect of impact loading and chemical corrosion on microdamage and crack propagation of white sandstone. The typical micro surfaces of the longitudinal section and fracture surface of the impact failure specimen are shown in Fig. 10.

The weak spot's presence of rock mass results in low strength properties of impact and irregular development of fractures. As shown in Fig. 9 (a) and (c), the micro-surface of these rock samples is uneven and rough, showing ups and downs, with small holes and fissures. Nevertheless, the fracture surface of (b) and (d) samples fluctuates slightly, accompanied by a fracture sheet structure. However, the longitudinal section of the specimen has no interfacial friction effect and the surface is rough. The shear plane of "X" shaped has interfacial friction, which leads to the improvement of fracture roughness under impact loading. The sandstones (e) and (g) had scattered and disordered particles or dominantly irregular grain boundaries, which shows the heterogeneity of the specimen and the defects of internal mineral lattice. The fracture surface of sandstones (f) and (h) is broken, and the rock is disordered, but there is a smooth surface locally. This is due to their mineralogical composition, which result in high strength against shear.

The type of chemical solution is closely related to the damage of rock microstructure [26]. Comparing the micro-surface of (a), (b) with (c), (d), it is found that the corrosion damage degree of Na_2SO_4 solution is greater than that of NaCl solution. Main performance: (a), (b) surface is rougher and better integrity than(c), (d). In addition to the hydraulic dissolution of sandstone soluble components, $SO4^{2-}$increase the pore water pressure of white sandstone specimen, deform and displace the rock particles to damage structure. The chemical reaction of some reaction zones to the interior of white sandstone is promoted, causing cracking damage [27]. In pore water, pore water chemical effect of Cl^- is small, and the damage degree is small.

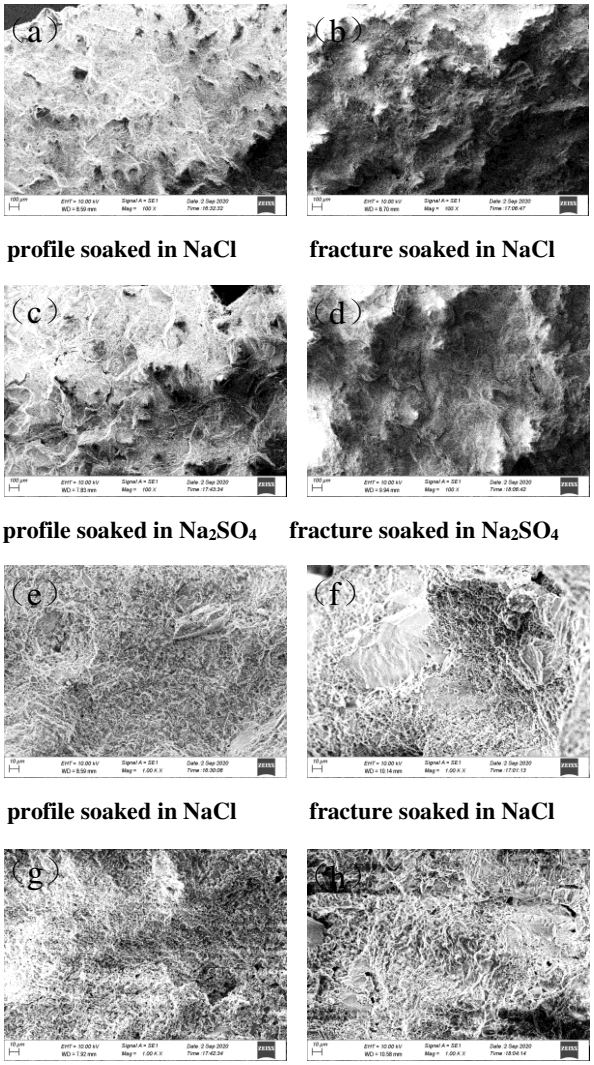

（a）～（d）are 100 times,（e）～（f）are 1000 times

Fig. 10 SEM images of impact sandstone in different solutions

4 Conclusions

In the present study, a series of cyclic impact tests were performed on white sandstone soaked in different hydrogen ion concentration solution sand with different axial pressures. The following conclusions are drawn:

1)The total cyclic impact number of sandstones that can withstand the loading gradually decreased with the polarization of the hydrogen ion concentration index of the solution under the same axial pressure. When the hydrogen ion concentration index of the solution is 7, the total cyclic impact number and stress peak of the sandstone specimens both became larger, and the rock samples responded with a significantly high resistant strength;

2) With increased the number of cycle impact, the transmission coefficient of stress wave propagating in the specimen gradually decreased under the same axial pressure. However, the reflection coefficient showed a trend of "first decrease and then increase".

3) Under the axial pressure of 6.3Mpa, the stress peak of sandstone resisting cyclic impact showed a trend of "stable in the early stage and then sharp decline ". Compared with axial pressure of 6.3Mpa, the stress peak of the sandstone was lower upon dynamic loading under an axial pressure of 12.6Mpa and 20.5MPa; when the sandstone had axial pressure of 26.8Mpa, the cyclic impact times of sandstone was few and the dynamic stress peak value was small.

4）The vertical section and fracture surface damage degree of white sandstone soaked in Na_2SO_4 solution is more serious than that in NaCl solution, and there are many fissures near the flake structure.

Acknowledgments

The authors are grateful for financial support from the National Natural Science Foundation of China (No.51664016, No.51664017) and Postgraduate Innovation Special Fund Project Jiangxi Province (ZS2020-S093).

Disclosure statement

No potential conflict of interest was reported by the authors.

References

[1] Liu Hongshuai, Bo Jingshan, Liu Dedong. Review on seismic stability analysis of rock and soil slopes[J]. Earthquake Engineering and Engineering Vibration, 2005 (01): 164-171.

[2] Li Diyuan, Cheng Tengjiao, Zhou Tao, et al. Experimental study on dynamic mechanical failure characteristics of marble with holes under impact Loading[J]. Chinese Journal of Rock Mechanics and Engineering, 2015, 02(2):249-260.

[3] Lin Daneng, Chen Shouru. Experimental study on rock damage law under cyclic impact loading[J]. Chinese Journal of Rock Mechanics and Engineering, 2005(22):4094-4098.

[4] Ju Yang, Wang Huijie, Yang Yongming, Hu Qinang, PENG Rui-Dong. Numerical simulation of mechanisms of deformation, failure and energy dissipation in porous

rock media subjected to wave stresses[J]. Science China-Technological Sciences,2010,53(4).

[5] Li Diyuan, Qiu Jiadong, Li Xibing. Study on dynamic tensile and compressive properties of layered sandstone under impact loading[J]. Chinese Journal of Rock Mechanics and Engineering,2015,34(10):2091-2097.

[6] Lin Yun, Zhou Keping, Li Jielin, Ke Bo, Gao Rugao. Weakening Laws of Mechanical Properties of Sandstone Under the Effect of Chemical Corrosion[J]. Rock Mechanics and Rock Engineering,2020, 53(3).

[7] Li Xibing, Zhou Zilong, Ye Zhouyuan, et al. Study on the mechanical properties of rock combined with dynamic and static loading[J]. Chinese Journal of Rock Mechanics and Engineering, 2008(07):1387-1395.

[8] Hu Jian, Gong Fengqiang, Jia Hangyu. Study on mechanics and energy dissipation characteristics of red sandstone in SHPB compression test[J]. Gold Science and Technology,2020,28(03):411-420.

[9] Gong Fengqiang, Wu Wuxing, Li Tian-bin, et al. Experimental simulation study on slab crack failure of surrounding rock in deep hard rock rectangular tunnel[J]. Rock and Soil Mechanics,2019,40(06):2085-2098.

[10] Jin Jiefang, Li Xibing, Wang Guanshi, et al. Failure mode and mechanism of sandstone under cyclic impact loading[J]. Journal of Central South University(Science and Technology),2012,43(04):1453-1461.

[11] Yin Tubing, Shu Ronghua, Li Xibing, WANG Pin, DONG Long-jun. Combined effects of temperature and axial pressure on dynamic mechanical properties of granite[J]. Transactions of Nonferrous Metals Society of China,2016,26(8).

[12] Tang Liansheng, Zhang Pengcheng, Wang Sijing. Experimental study on rock fracture mechanics effect of water-rock chemical action [J]. Chinese Journal of Rock Mechanics and Engineering,2002(06):822-827.

[13] Li Guanglei, Wei Liyuan, Su Haijian, et al. Study on the impact dynamics performance of chemically corroded limestone SHPB[J]. Chinese Journal of Rock Mechanics and Engineering, 2012,37(09):2075-2083.

[14] Wu Yun. Study on mechanical properties and rock burst mechanism of acidified rock under combined action of dynamic and static [D]. East China Jiao tong University,2017.

[15] Feng Xiating, Chen Sili, Li Shaojun. Effects of water chemistry on microcracking and compressive strength of granite[J]. International Journal of Rock Mechanics and Mining Sciences,2001,38(4).

[16] Bieniawski Z T, Hawkes I. Suggested Methods for Determining Tensile Strength of Rock Materials[J]. International Journal of Rock Mechanics and Mining Sciences and Geomechanics Abstracts, 1978, 15(3):99-103.

[17] Zhao Guangming, Ma Wenwei, Meng Xiangrui. Failure mode and energy characteristics of rock materials under dynamic load [J]. Rock and Soil Mechanics, 2015,36 (12): 3598-3605 + 3624.

[18] Tang Chaosheng, Shi bin, Wang Baojun. Analysis of influencing factors in soil microstructure based on SEM [J]. Chinese Journal of Geotechnical Engineering, 2008 (04): 560-565.

[19] Mohr D, Gary G, Lundberg B. Evaluation of Stress-strain Curve Estimates in Dynamic Experiments[J]. International Journal of Impact Engineering, 2010, 37(2):161-169.

[20] Chai Shaobo, Wang Hao, Jing Yanlin, et al. Experimental study on dynamic compression characteristics of cumulative damage of filled jointed rock[J]. Chinese Journal of Rock Mechanics and Engineering, 2020,39 (10): 2025-2037.

[21] Barton N, Bandis S, Bakhtar K. Strength, deformation and conductivity coupling of rock joints[J]. International Journal of Rock Mechanics and Mining Sciences and Geomechanics Abstracts,1985, 22(3):121-140.

[22] Wang Weihua, Li Xibing, Zuo Yujun. Influence of nonlinear normal deformation joint on elastic P-wave propagation[J]. Chinese Journal of Rock Mechanics and Engineering, 2006 (06): 1218-1225.

[23] Zhu Jingjing, Li Xibing, Gong Fengqiang, et al. Dynamic characteristics and damage law of sandstone under impact loading[J]. Journal of Central South University (Science and Technology),2012,43(07):2701-2707.

[24] Jin Jiefang, Wu Yue, Zhang Rui, et al. Impact velocity and axial static loading under the influence of red sandstone fragmentation and energy consumption[J]. Explosion and Shock Waves,2020,40(10):42-55.

[25] Xu J. Debris slope stability analysis using three-dimensional finite element method based on maximum shear stress theory[J]. Environmental Earth Sciences, 2011, 64(8):2215-2222.

[26] Tang Liansheng, Zhang Pengcheng, Wang Sijing. Experimental study on macroscopic mechanical effect of rock under water-rock chemical action[J]. Chinese Journal of Rock Mechanics and Engineering,2002(04):526-531.

[27] Han Tielin, Chen Yunsheng, Shi Jun-ping, et al. Experimental Study on the influence of hydrochemical corrosion on the mechanical properties of sandstone[J]. Chinese Journal of Rock Mechanics and Engineering, 2013(S2):003064-3072.

Figures

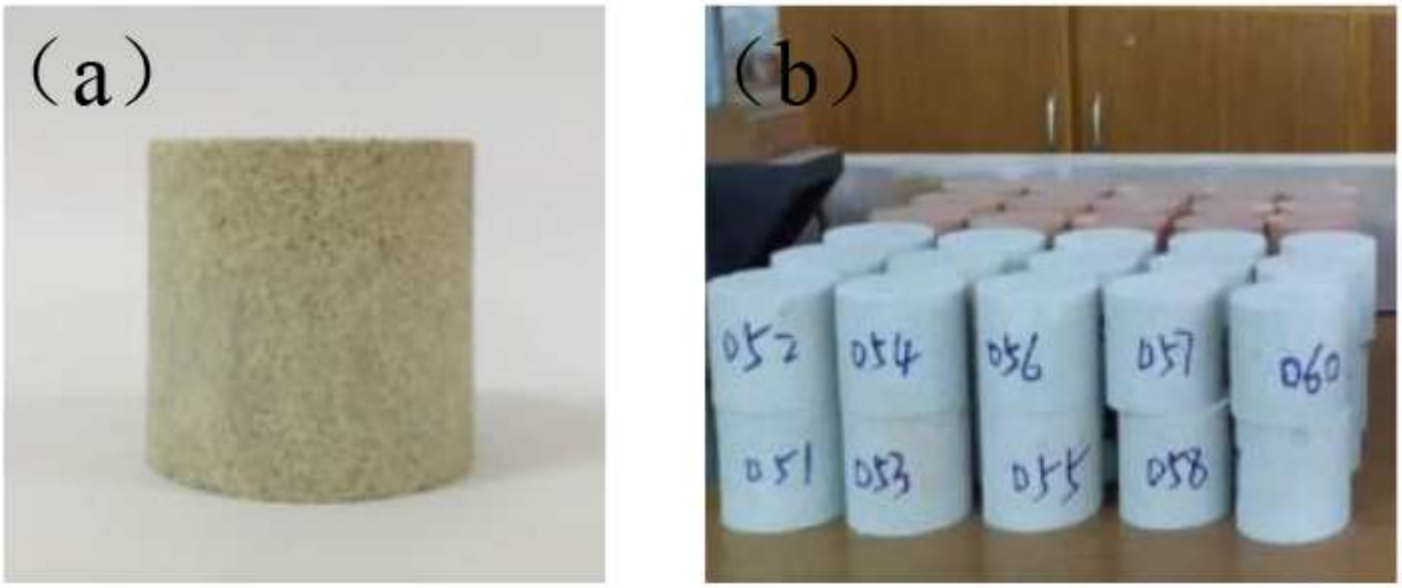

Figure 1

White sandstone specimens

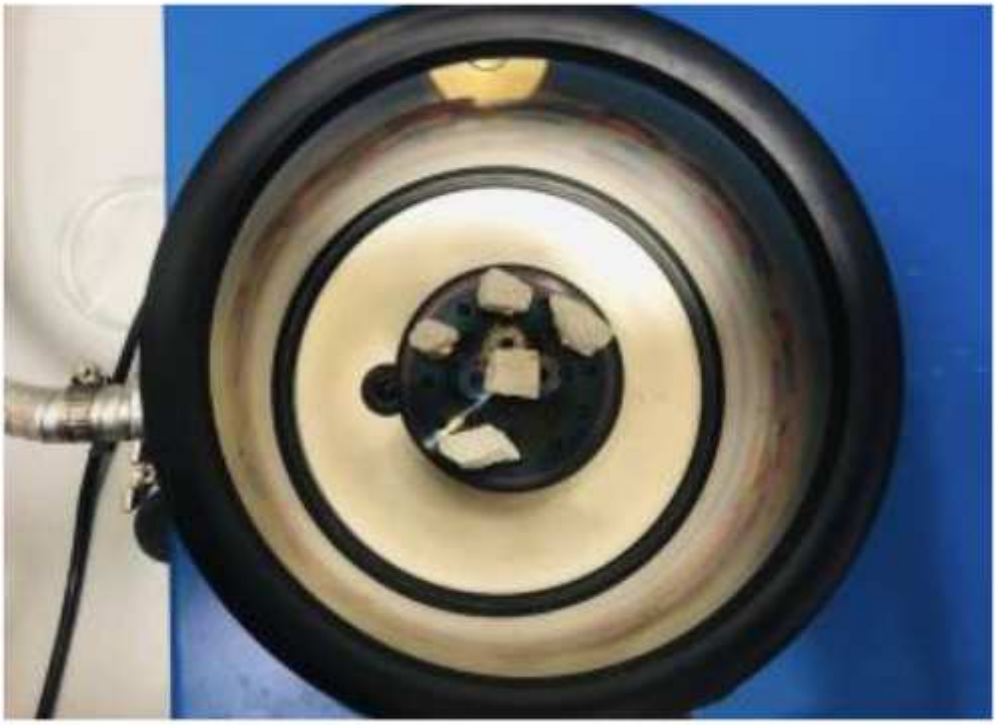

Figure 2

Scanning electron microscope of samples

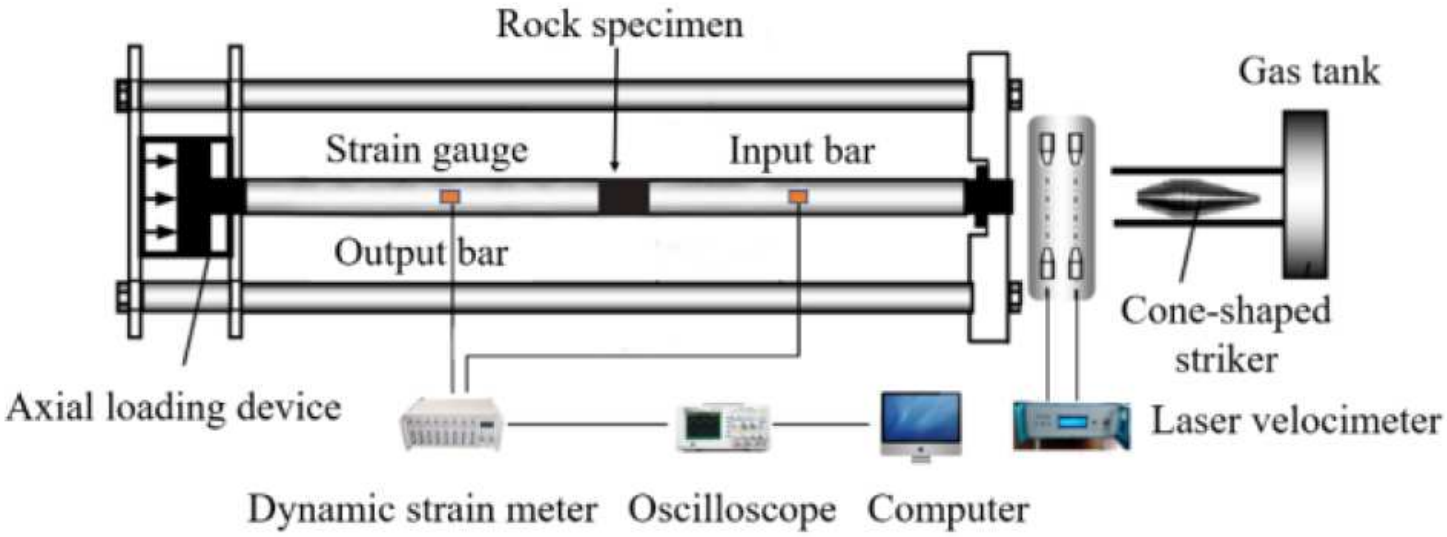

Figure 3

Diagram of SHPB testing apparatus

Figure 4

Scanning electron microscopy

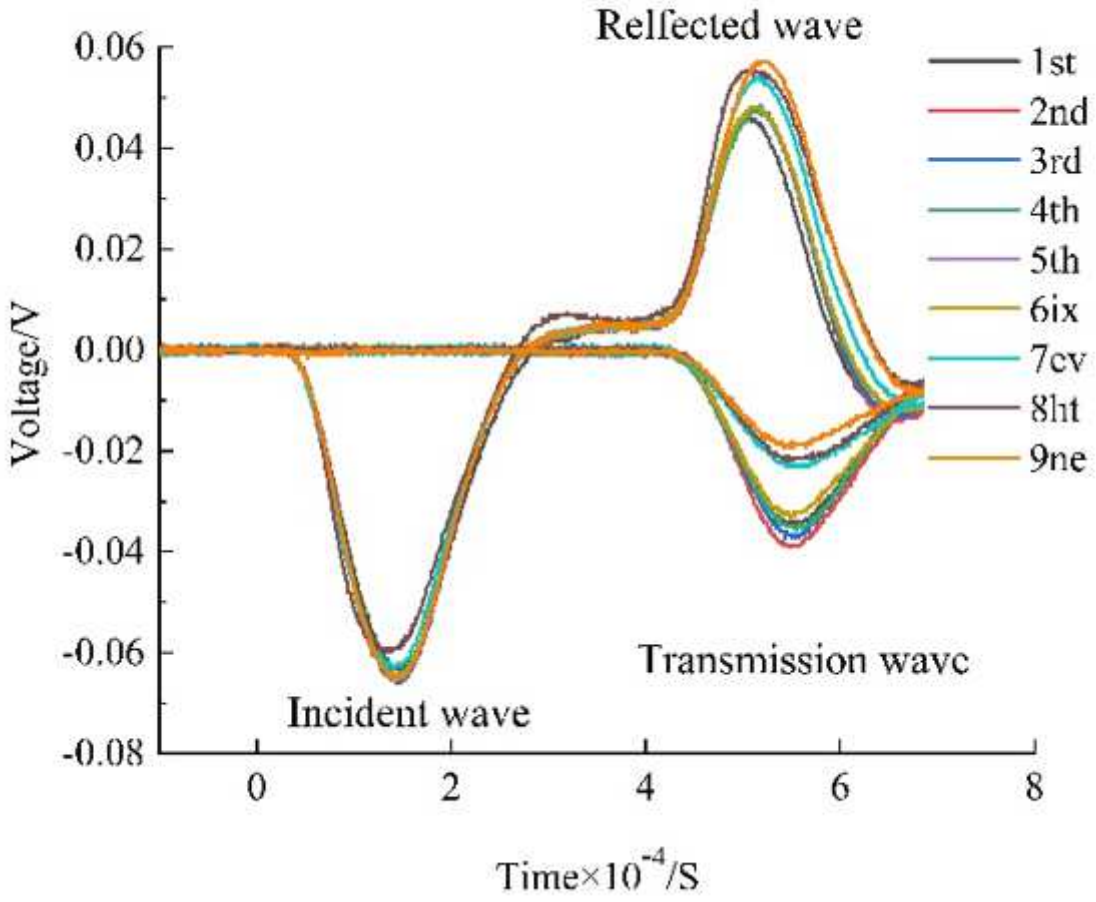

Figure 5

Stress wave superposition diagram of w-033

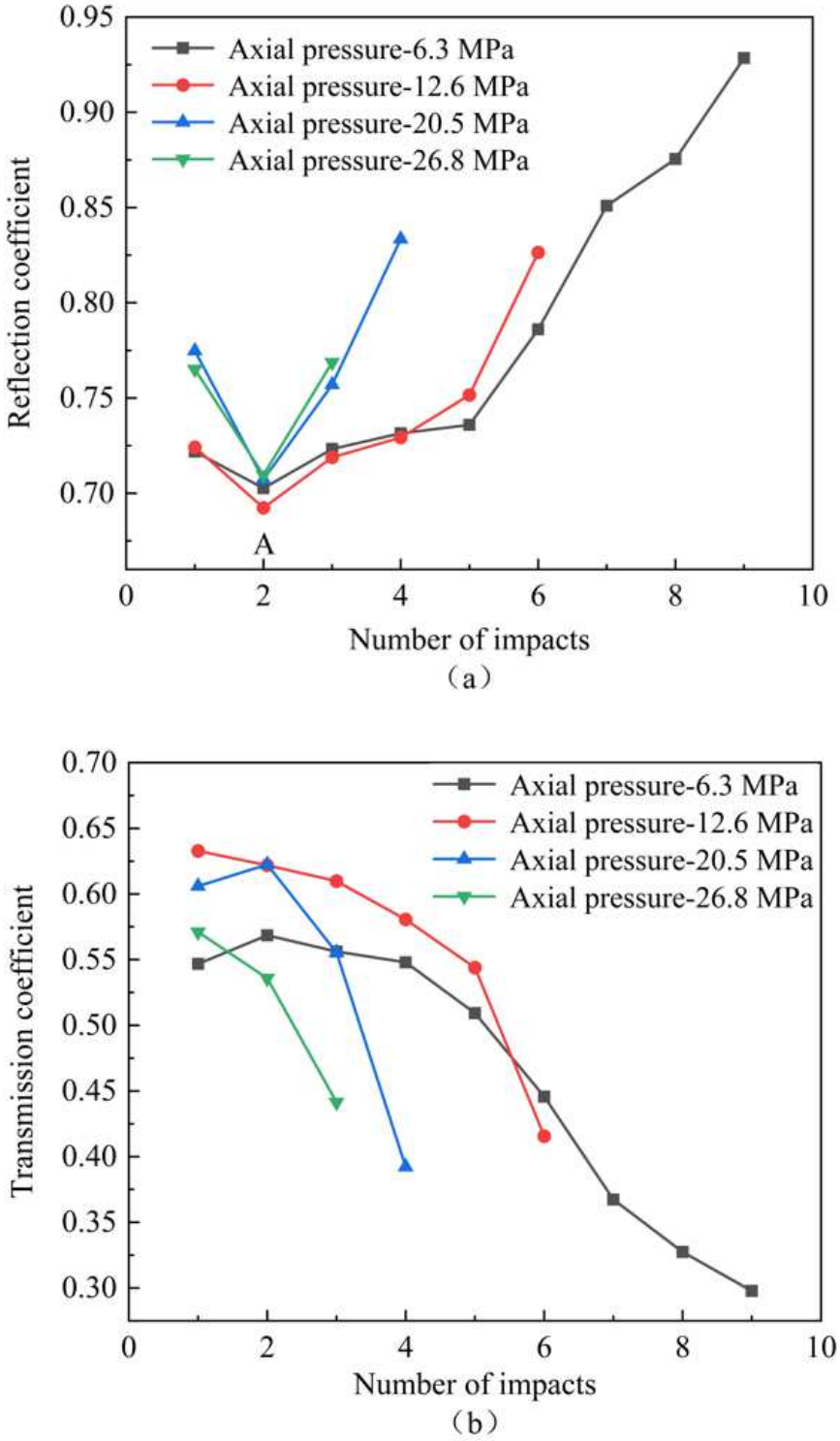

Figure 6

Trend chart of transmission and reflection coefficient

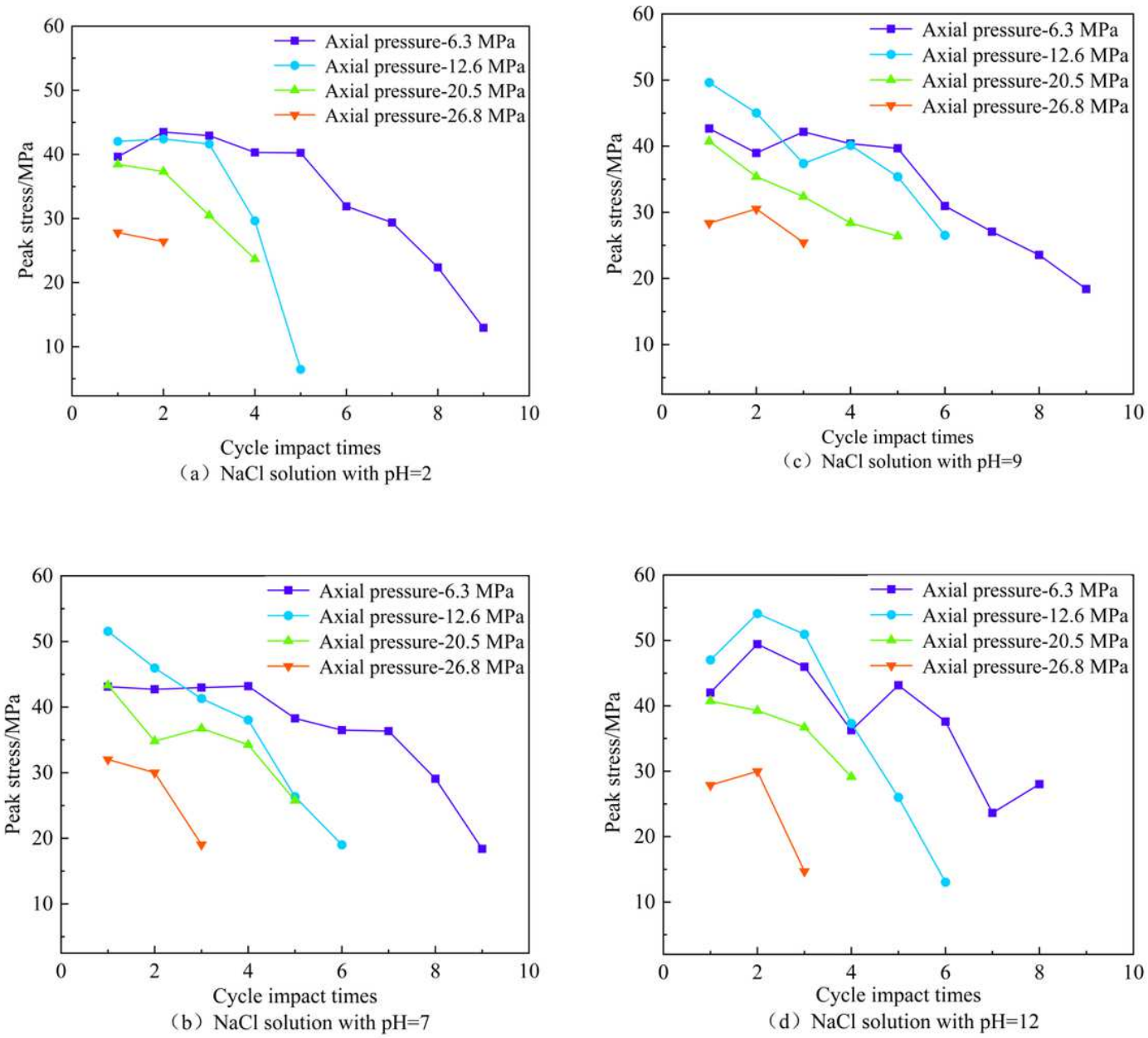

Figure 7

Relationship between peak stress and the number of impacts under different axial pressures

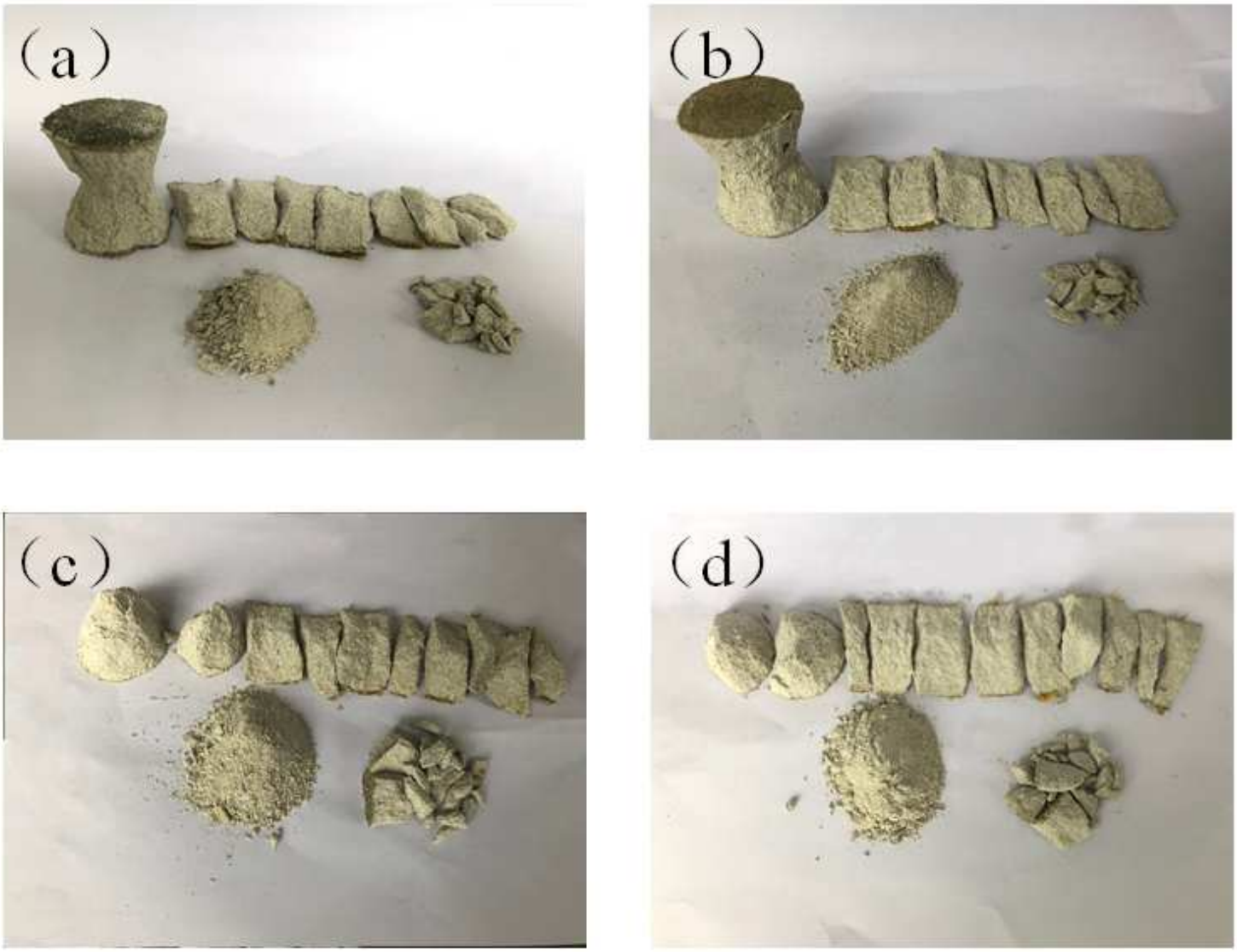

Figure 8

Failure mode of samples

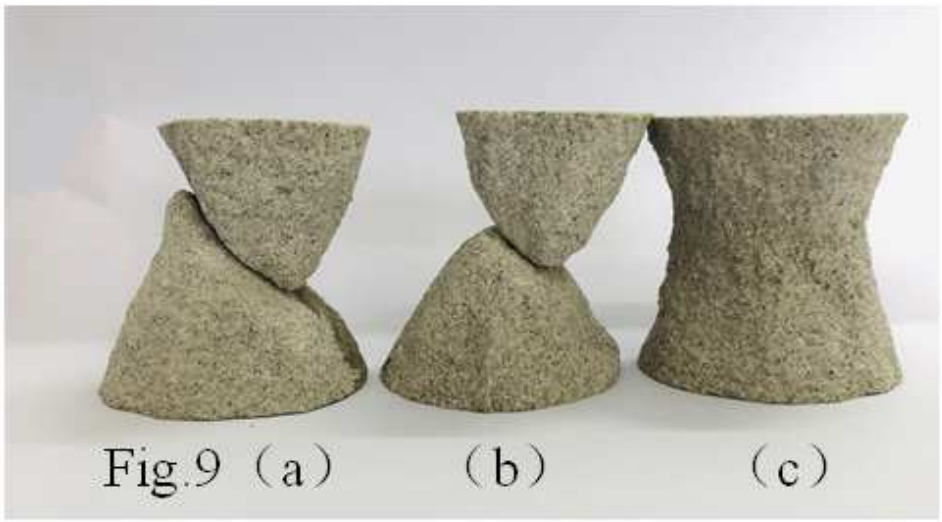

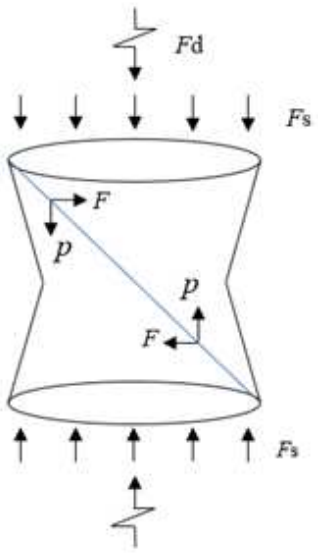

Figure 9

Failure modes and force condition of rocks

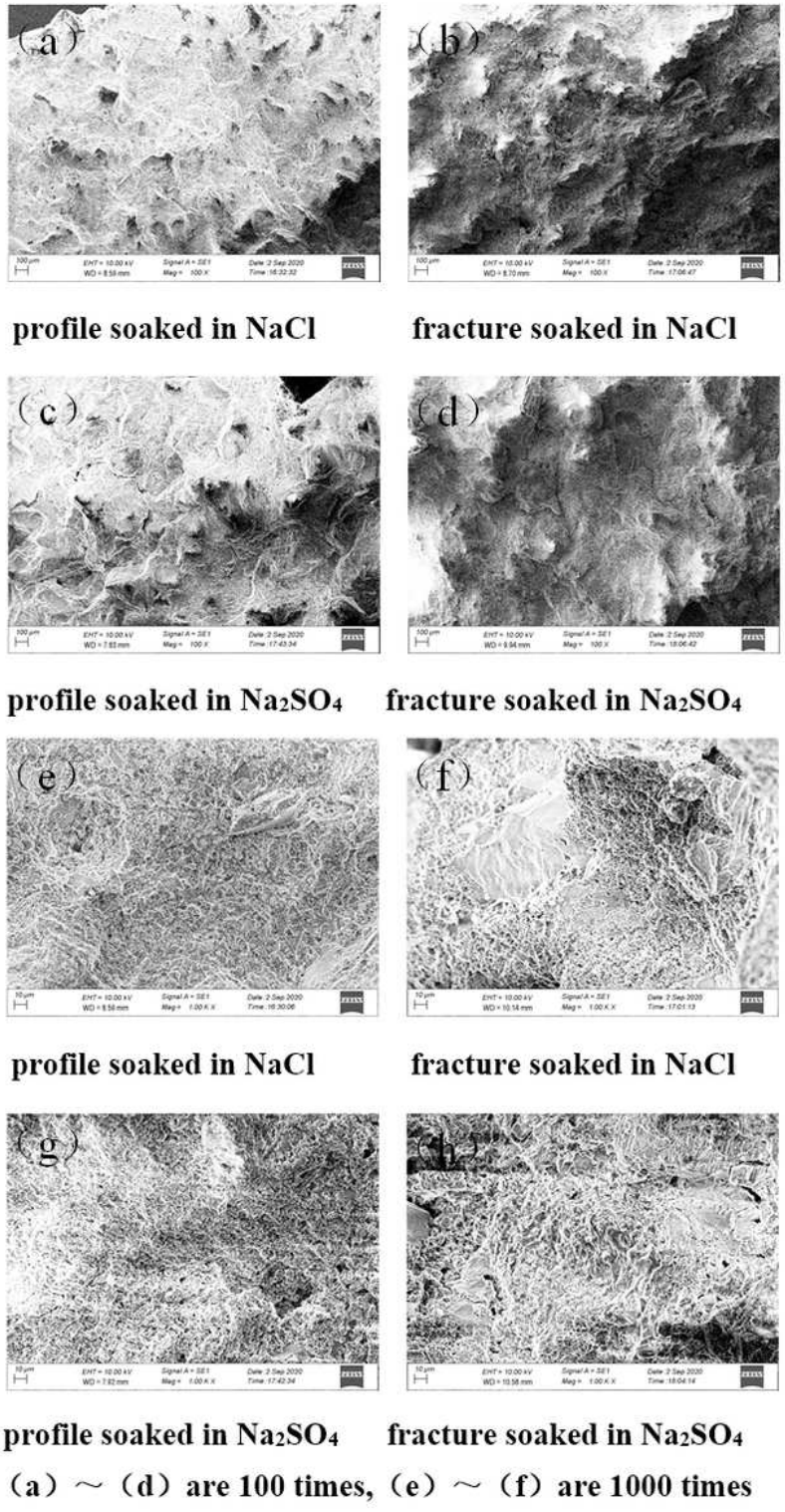

Figure 10

SEM images of impact sandstone in different solutions